Journal of Hydrology, 125 (1991) 1–24
Elsevier Science Publishers B.V., Amsterdam

[2]

ANALYTICAL MODELING OF A FRACTURE ZONE IN THE BRULE FORMATION AS AN AQUIFER RECEIVING LEAKAGE FROM WATER-TABLE AND ELASTIC AQUITARDS

WARREN BARRASH[1] and DALE R. RALSTON[2]

[1]*INEL Oversight Program, Idaho Department of Health and Welfare, 1410 N. Hilton Rd., Boise, ID 83706 (U.S.A.)*
[2]*Department of Geology and Geological Engineering, University of Idaho, Moscow, ID 83843 (U.S.A.)*

(Received 28 July 1990; accepted after revision 30 September 1990)

ABSTRACT

Barrash, W. and Ralston, D.R., 1991. Analytical modeling of a fracture zone in the Brule Formation as an aquifer receiving leakage from water-table and elastic aquitards. J. Hydrol., 125: 1–24.

Hydrostratigraphic data define a subhorizontal, laterally limited, highly permeable zone of intensely fractured siltstone (major fracture zone) within the relatively impermeable Brule Formation at a site in Cheyenne County, Nebraska. Two types of transient hydraulic responses were noted in 11 observation wells during an eight-day aquifer test: Type 1 responses occurred in wells which intercepted the major fracture zone; Type 2 responses occurred in wells outside the major fracture zone.

Transient responses in Type 1 observation wells are matched with type curves for a three-layered system with a water-table aquitard above an aquifer (major fracture zone) which overlies an elastic aquitard. Because the aquifer is laterally limited and the Brule Formation beyond the major fracture zone has finite hydraulic conductivity, real late-time behavior falls between type curves for an infinite aquifer and for an aquifer with an impermeable boundary at reasonable distances from the pumping well. Aquifer and aquitard parameters determined from curve matches with both limiting boundary conditions are identical for inner-ring observation wells, and nearly so for middle-ring observation wells. Outer-ring observation wells exhibited Type 2 responses which were used only to identify the extent of the major fracture zone.

INTRODUCTION

The Brule Formation is a siltstone unit that is used as an aquifer in the High Plains (western Nebraska, eastern Wyoming, northeastern Colorado) where younger Tertiary units are thin, unsaturated or eroded away. In places, groundwater development for irrigation from the Brule Formation has resulted in long-term water-level declines, abandonment of shallow wells, well interference, and seasonal supply problems. Because the Brule Formation is dominantly siltstone, groundwater yields adequate for irrigation are possible only where wells intercept highly conductive secondary permeability zones.

0022-1694/91/$03.50

NOTATION

In the text, parameters specific to a given hydrostratigraphic unit are designated as follows: ′ denotes aquitard overlying the aquifer, ″ denotes aquitard underlying the aquifer, no mark denotes the aquifer or geological material not specified as part of an aquifer or aquitard

---

b = thickness of hydrostratigraphic unit, L.
h = head, L.
h_0 = initial head, L.
$\bar{h}_D$ = Laplace transform line-source solution for dimensionless head in the aquifer.
I_0 = modified Bessel function of the first kind and order zero.
I_1 = modified Bessel function of the first kind and order one.
K = hydraulic conductivity, L T^{-1}.
K_r = horizontal (radial) hydraulic conductivity, L T^{-1}.
K_z = vertical hydraulic conductivity, L T^{-1}.
K_0 = modified Bessel function of the second kind and order zero.
K_1 = modified Bessel function of the second kind and order one.
L = thickness of capillary fringe, L.
p = Laplace transform variable.
q = leakage source term, L^3 T^{-1}.
Q = pumping discharge rate, L^3 T^{-1}.
r = distance from pumping well to observation well, L.
r_w = radius of pumping well, L.
Ss = specific storage, L^{-1}.
Sy = specific yield.
t = time, T.
z = vertical dimension in aquitard, L.
τ = time, where $\tau < t$, T.

Dimensionless parameters

$$h_D = \frac{4\pi Kb}{Q}(h_0 - h)$$

$$r_D = r/r_w$$

$$R_D = r/r_w$$

$$t_D = \frac{Kt}{Ssr_w^2}$$

The hydrostratigraphic setting and hydraulic behavior of one highly conductive secondary permeability zone in the Brule Formation was investigated in Sidney Draw, Cheyenne County, Nebraska (Fig. 1). The hydrostratigraphic setting was interpreted from: (1) electric logs of oil and gas wells; (2) drillers' logs from irrigation wells; (3) drilling, core, and geophysical logs from test wells at the study site (Barrash and Morin, 1985, 1987; Barrash, 1986; Morin and Barrash, 1986).

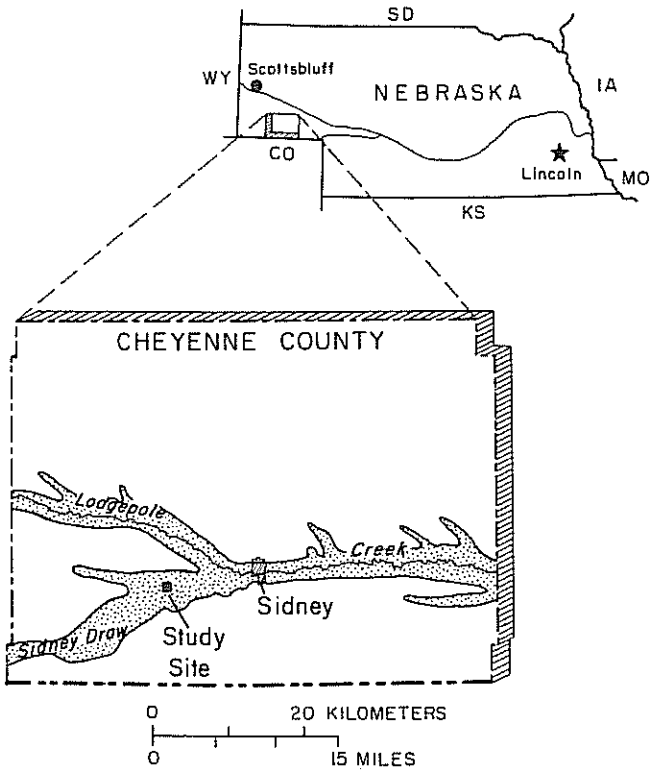

Fig. 1. Location of study area in Sidney Draw, Cheyenne County, Nebraska.

The hydraulic behavior of the highly conductive secondary permeability zone (major fracture zone) is interpreted from results of an eight-day aquifer test during which drawdown was monitored in the pumping well and in 11 observation wells. In this paper we present a brief description of the hydrostratigraphic setting of the major fracture zone, we describe the eight-day aquifer test, and we use an analytical model with two limiting boundary conditions to interpret the aquifer-test results in a manner consistent with hydrostratigraphic data.

HYDROSTRATIGRAPHIC SETTING

At the study site, the Brule Formation is predominantly siltstone with thin ($\leqslant 1.2$ m) beds of claystone and sandstone. Lithologic features observed in core that influence groundwater flow include several types of pedotubules, subhorizontal parting planes (Fig. 2a–d), and perhaps subvertical joints (Barrash, 1986) which are inferred to be present on the basis of a regional, linear,

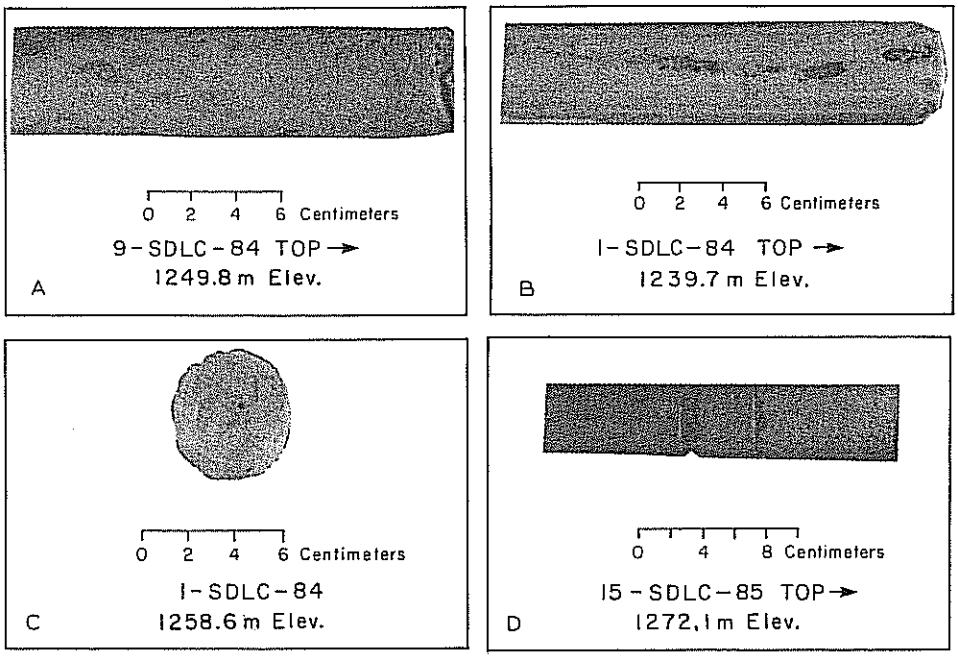
0 2 4 6 Centimeters
9-SDLC-84 TOP
1249.8 m Elev.
A
0 2 4 6 Centimeters
1-SDLC-84 TOP
1239.7 m Elev.
B
0 2 4 6 Centimeters
1-SDLC-84
1258.6 m Elev.
C
0 4 8 Centimeters
15-SDLC-85 TOP
1272.1 m Elev.
D

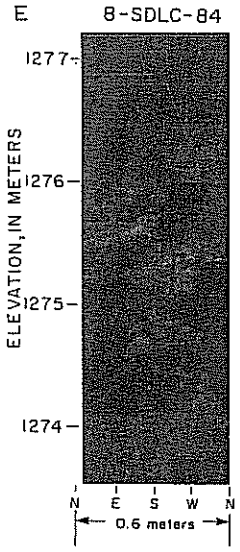
E
8-SDLC-84
1277
1276
1275
1274
ELEVATION, IN METERS
N E S W N
0.6 meters

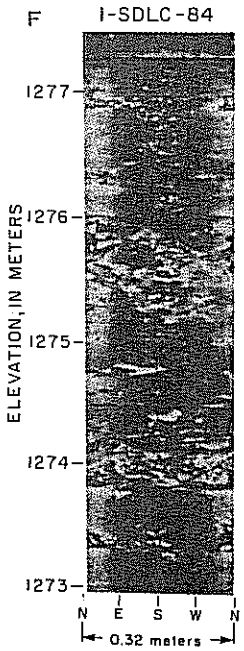
F
1-SDLC-84
1277
1276
1275
1274
1273
ELEVATION, IN METERS
N E S W N
0.32 meters

topographic fabric. Additional details and discussion of Brule Formation stratigraphy is given in Barrash (1986).

The major fracture zone is a subhorizontal, laterally limited, hydrostratigraphic unit which is present below the water table and which can be traced across the central portion of the study site (Fig. 3) by drilling experience (lost circulation) and geophysical logs (Barrash and Morin, 1985, 1987; Barrash, 1986). The major fracture zone ranges in thickness from 1 to 4 m (average = 2.3 m) and consists of one intensely fractured layer or several thin layers in close vertical proximity. Diameters of blocks bounded by fractures range from 0.5 to 15 cm; diameters of 1.3 cm are common (Fig. 2e–f).

The major fracture zone was not recognized in the northeastern part of the study site (Well 9-SDLC-84) or to the northwest (Well G11709) (Fig. 3).

AQUIFER TEST

An eight-day aquifer test was conducted from September 25 to October 3, 1984. Eleven observation wells surrounded the pumping well (G3027) in three groups or 'rings' at succesively greater radial distances from G3027 (Fig. 4). Water produced during this test was applied through gated pipe to an alfalfa field $\sim$500 m east of G3027.

Water levels were monitored in all 12 wells prior to the test to determine trends. A rising trend was observed because the irrigation season had ended recently for most crops. However, the trend also included the effects of a pumping irrigation well $\sim$1100 m southeast of G3207 (Fig. 4). Drawdown in the test wells was adjusted to remove the combined trend effects during the test. Values of elapsed time, measured drawdown and adjusted drawdown are given elsewhere (Barrash, 1986).

Pumping well

The initial pumping rate at G3207 (during the first 2.5–4 min) probably exceeded the long-term average (3.4 $m^3 min^{-1}$, or 900 gallons per min.). The initial drawdown in G3207 was followed by *decreasing* drawdowns until 2.5–4 min (Fig. 5). Discharge from G3207 was pumped into an initially empty conduit system for delivery to the alfalfa field east of the study site (Fig. 4). Because initial pumping was only against atmospheric pressure in the empty

Fig. 2. Core segments and televiewer images that exhibit secondary permeability features from the Brule Formation at the study site. (A) Subvertical, branching pedotubule filled with coarser-grained material than occurs in the surrounding matrix. (B) Open, subvertical pedotubule. (C) Plan view of siltstone with an open, subvertical pedotubule. (D) Parting planes in siltstone. (E) Televiewer image: fracture zone has a distinct top and bottom; dark patches are regions of greater well diameter. (F) Televiewer image: 'layers' of intensely fractured siltstone separated by unfractured siltstone.

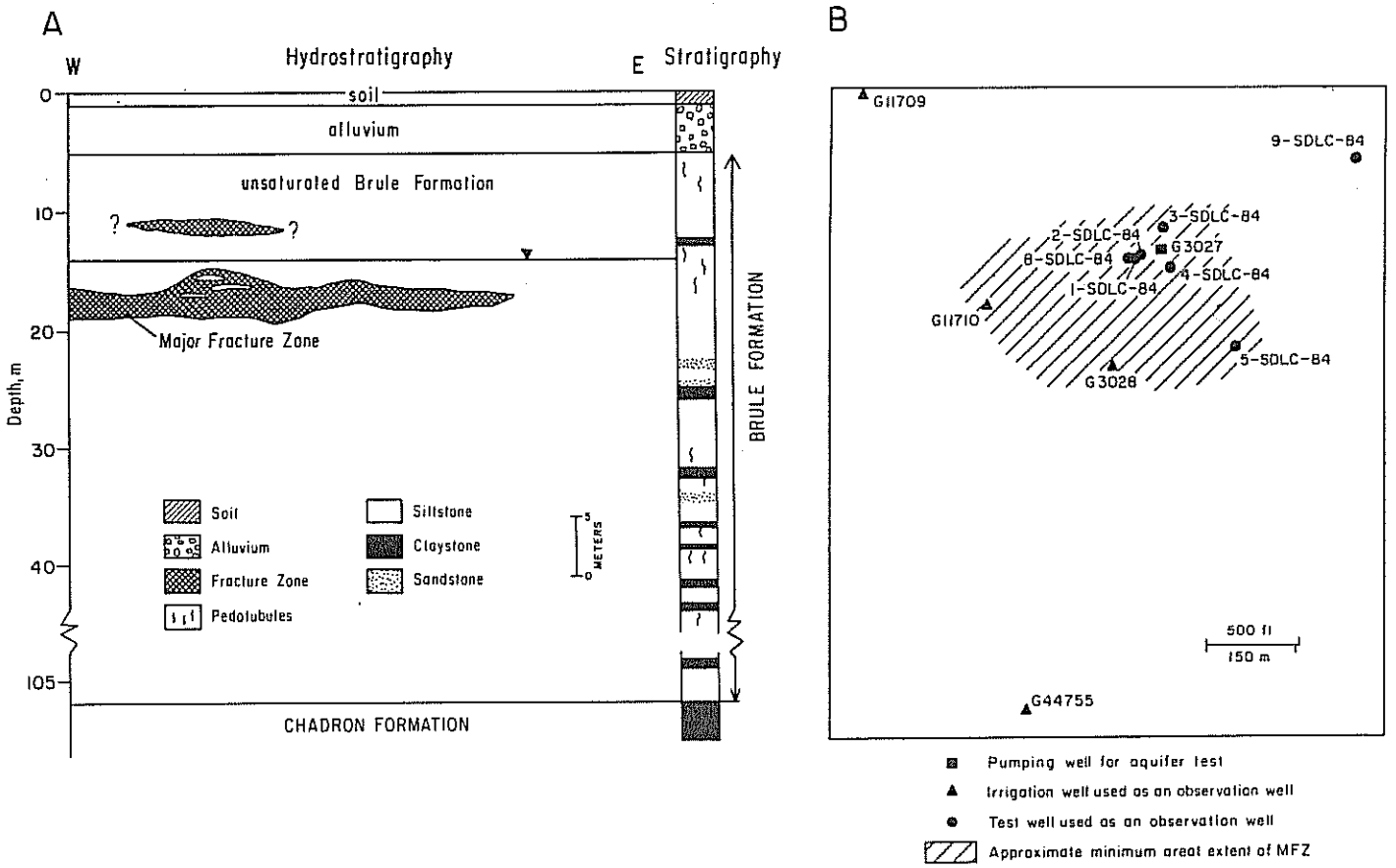

Fig. 3. (A) Generalized hydrostratigraphy at the study site. (B) Interpreted minimum areal extent of the major fracture zone at the study area.

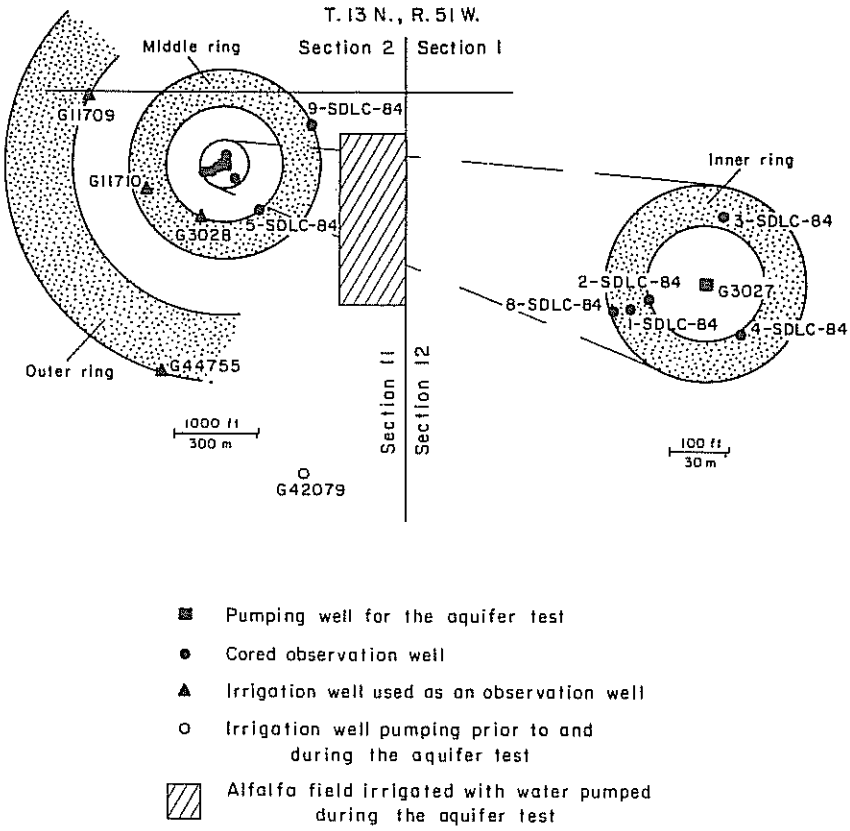

Fig. 4. Well configuration for the large-scale aquifer test. Pumping Well G3027 is surrounded by 11 observation wells distributed at three ranges of distance from G3027: inner-, middle-, and outer-ring wells.

pipe, and then progressively against a filling conduit, the drawdown pattern represents a progressively decreasing pumping rate until the conduit system filled and subsequent pumping was against a constant head.

After the initial period of decrease, drawdown increased slowly until 30–40 min when it increased at an increasing rate. No linear semi-logarithmic relationship between drawdown and log time is apparent at late time. Final drawdown in G3207, adjusted for the rising water-level trend, was 2.31 m at the end of about eight days of pumping (Fig. 5).

Observation wells

Observation wells exhibited two types of water-level or adjusted drawdown responses. Type 1 response occurred in observation Wells 1-, 2-, 3-, 4-, 5-, and 8-SDLC-84, G3208, and G11710, all of which are < 300 m from the pumping well

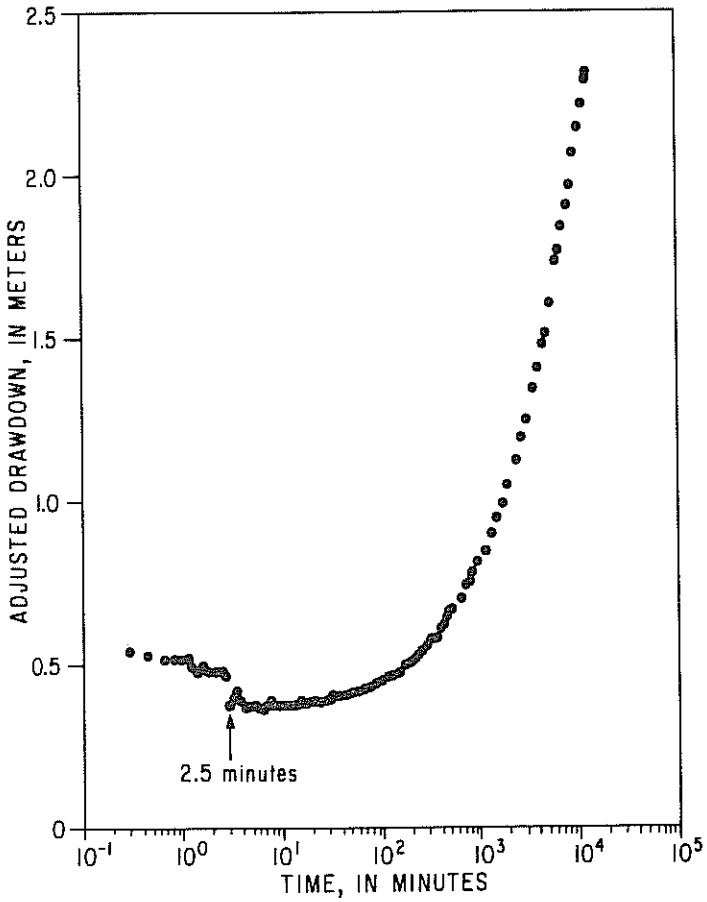

Fig. 5. Semi-log adjusted drawdown plot for the pumping Well G3027. During the first 2.5 min of the test, the pumping rate was greater than the (constant) pumping rate for the remainder of the test.

(Fig. 4). All Type 1 wells had the same rising, pre-test water-level trend of 1.5×10^{-5} m min^{-1}. Type 1 wells have the following similar behavior: (1) initial drawdown at $\leqslant 3$ min after pumping started; (2) similar adjusted drawdowns at any given time during the pumping test (Table 1); (3) measurable water-level recovery in < 10 min in all Type 1 wells that were monitored when the pump was shut off.

Type 2 responses occurred in Wells 9-SDLC-84, G11709, and G44755, which are > 300 m from G3027 (Fig. 4). Pre-test water-level trends ranged from zero to 2×10^{-5} m min^{-1}. During the test, Type 2 wells showed (Fig. 6): (1) no measurable drawdown for < 5.6–28 h; (2) 'S'-shaped(?) log–log adjusted drawdown curves; and (3) delay in recovery for hours after pumping ceased. Also, maximum adjusted drawdowns ranged from 0.17 to 0.84 m in Type 2 wells.

TABLE 1

Adjusted drawdown (in meters[a]) at Type 1 wells and G3027 at selected time intervals

Time (min)	G3027 (r = 0.3 m)	2-SDLC-84 (r = 31 m)	4-SDLC-84 (r = 34 m)	3-SDLC-84 (r = 37 m)	1-SDLC-84 (r = 43 m)	8-SDLC-84 (r = 51 m)	5-SDLC-84 (r = 203 m)	G3028 (r = 203 m)	G11710 (r = 294 m)
5	0.38	0.067	0.073	0.085	0.061	0.049	0.006	0.034	—[b]
100	0.46	0.16	0.16	0.18	0.17	0.15	0.094	0.11	—[b]
500	0.68	0.36	0.38	0.39	0.40	0.36	0.30	0.32	0.32
1000	0.84	0.56	0.55	0.58	0.57	0.53	0.49	0.50	0.49
5000	1.66	1.36	1.34	1.37	1.32	1.35	1.25	1.29	1.28
11275	2.31	1.98	1.99	2.00	2.07	1.97	1.91	1.94	1.96

[a]Tabled values are either measured or linearly interpolated.
[b]Early data unavailable owing to mechanical failure.

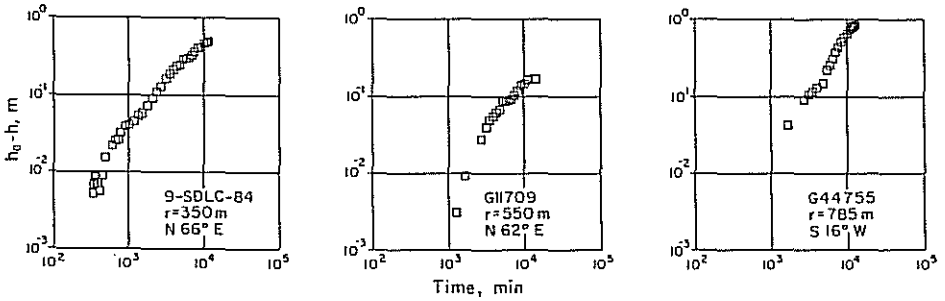

Fig. 6. Log–log adjusted drawdown curves for Type 2 ($r > 300$ m) observation wells. Radial distance, r, and azimuth for each well are in relation to G3027.

THREE-LAYER HYDROSTRATIGRAPHIC SYSTEM

Interpretation of hydrostratigraphic data indicates that the major fracture zone is a subhorizontal, laterally limited, highly permeable zone of densely fractured siltstone within a relatively low hydraulic conductivity ($K_r' \simeq 10^{-6}\,\mathrm{m\,s^{-1}}$) section of the Brule Formation (Barrash, 1986; Barrash and Morin, 1987). At the time of the aquifer test, the major fracture zone was 0.9–2.9 m below the water level in observation wells open above, through, and below the major fracture zone. Therefore, where the major fracture zone occurs, the Brule Formation may be conceptualized as a three-layer system with an aquifer sandwiched between a water-table aquitard and an elastic aquitard.

System characteristics and assumptions

System characteristics and assumptions used in testing the conceptual model against aquifer-test data are given schematically in Fig. 7 and are discussed below. Symbols used are identified in the Notation section. Sensitivity analysis is discussed after model development.

(1) The major fracture zone is treated as an aquifer with an average thickness of 2.3 m. Criteria for assessing whether a fractured medium behaves like a porous medium have been discussed by Long et al. (1982). The major fracture zone has a high density of fractures in non-uniform orientation distribution, and fracture lengths are short ($\ll 1$ m) relative to volumes available to achieve a statistically homogeneous sample of fractured material (Barrash, 1986; Barrash and Ralston, 1988). No data are available on fracture–aperture distribution.

(2) The three-layer model is based on the strong contrast in horizontal permeability between the major fracture zone and the relatively unfractured Brule Formation above and below (Barrash, 1986; Barrash and Morin, 1987).

(3) Although the aquifer is laterally limited and has uncertain shape in plan view, it is idealized first as a thin infinite layer and then as a thin circular

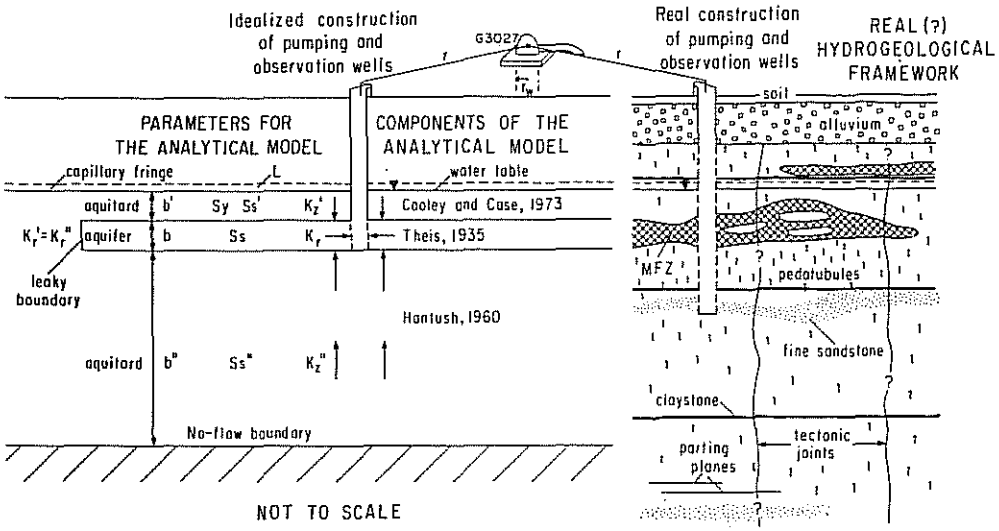

Fig. 7. Simplified conceptual and analytical three-layer models that are used to match behavior in the complex hydrogeological setting in Sidney Draw. Labeled parameters and dimensions which characterize the model are discussed in the text. In the coordinate system for analytical modeling, the origin for the radial coordinate, r, is at the axis of the pumping well, G3027. The vertical coordinate, z, is positive upward from the base of the lower aquitard.

cylinder. For the case of a thin circular cylinder, the analytical model assumes the pumping well is at the center of the cylinder. This assumption is not supported by field evidence (Fig. 3b) although the complete, plan-view geometry of the fracture zone is not yet known.

(4) The aquifer is overlain by a water-table aquitard (saturated, unfractured Brule Formation).

(5) The aquifer is underlain by an elastic aquitard. Hydrostratigraphic data indicate ~ 107 m of Brule Formation are present between the major fracture zone and the less-permeable clays of the Chadron Formation. The lower boundary is assumed to be an impermeable boundary.

(6) As a first approximation, specific storage is taken to be equal in the water-table aquitard and in the aquifer. Although the major fracture zone has porosity due to both the fracture network and the intergranular porosity of siltstone blocks between fractures, porosity in the siltstone blocks is ~ 0.4 (Barrash, 1986). Therefore, the specific storage of the fracture network (as a fraction of the total specific storage of the fracture-plus-matrix total volume in the major fracture zone) is probably small compared with the specific storage of the siltstone matrix blocks (e.g. Barenblatt et al., 1960). Hence, specific storage in the major fracture zone is given the value calculated for shallow Brule Formation, $Ss = Ss' = 7.5 \times 10^{-5}\,\mathrm{m}^{-1}$; the calculated value for the middle of the lower aquitard is $Ss'' = 5 \times 10^{-5}\,\mathrm{m}^{-1}$ (Barrash, 1986).

(7) The capillary fringe is initially assigned a thickness of 0.6 m. This

assignment is based on observations of saturated Brule Formation siltstone above the water level at the margins of irrigation drains.

Analytical model

An analytical model is presented for a three-layer system of an aquifer receiving leakage from a water-table aquitard above and an elastic aquitard below that is bounded at its base by an impermeable boundary. The mathematical development includes the governing equations, initial conditions, upper and lower boundary conditions, and two limiting lateral boundary conditions (an infinite aquifer and an aquifer with an impermeable lateral boundary).

The equation for radial flow in the infinite aquifer, in cylindrical coordinates, is

$$\frac{\partial^2 h}{\partial r^2} + \frac{1}{r}\frac{\partial h}{\partial r} = \frac{Ss}{K_r}\frac{\partial h}{\partial t} + q' - q'' \tag{1}$$

where q' and q'', the source terms for leakage from the water-table aquitard and the elastic aquitard respectively, are

$$q' = -(K'_z/K_r b)(\partial h'/\partial z) \tag{2}$$

$$q'' = -(K''_z/K_r b)(\partial h''/\partial z) \tag{3}$$

The initial condition is

$$h = h_0 \qquad r > r_w \tag{4}$$

The boundary conditions are

$$\text{At } t > 0,\ h(\infty,t) = h_0 \tag{5}$$

$$\lim_{r \to 0} r\frac{\partial h(r,t)}{\partial r} = -\frac{Q}{2\pi K_r b} \tag{6}$$

The equation for vertical flow in the water-table aquitard (Cooley and Case, 1973) is

$$\frac{\partial^2 h'}{\partial z^2} = \frac{Ss'}{K'_z}\frac{\partial h'}{\partial t} \qquad b'' + b \leqslant z \leqslant b'' + b + b' \tag{7}$$

with the initial condition

$$h'(r,z) = h_0 \tag{8}$$

and with the boundary conditions, at $t > 0$,

$$h'(r,b'' + b) = h(r) \tag{9}$$

$$\frac{\partial h'(r,b'' + b + b')}{\partial z} = -\frac{\varepsilon Sy}{K'_z}\int_0^t \frac{\partial h'}{\partial \tau} e^{-\varepsilon(t-\tau)} dt \tag{10}$$

where

$$\varepsilon = \frac{K'_z}{SyL} \tag{11}$$

The equation for vertical flow in the lower aquitard with an impermeable lower boundary (Hantush, 1960) is

$$\frac{\partial^2 h''}{\partial z^2} = \frac{Ss''}{K''_z}\frac{\partial h''}{\partial t} \qquad 0 \leqslant z \leqslant b'' \tag{12}$$

where the initial condition

$$h''(r,z) = h_0 \qquad 0 \leqslant z \leqslant b'' \tag{13}$$

and with the boundary conditions, at $t > 0$,

$$h''(r,b'') = h(r) \tag{14}$$

$$\frac{\partial h''(r,0)}{\partial z} = 0 \tag{15}$$

Moench and Ogata (1984) used the Stehfest (1970) algorithm to perform the numerical inversion of the Laplace transform to solve both the cases of leakage from an aquitard with an impermeable boundary and of leakage from a water-table aquitard. These two solutions are combined to generate the type curves of h_D against t_D/r_D^2 that are used to match with the log–log adjusted drawdown behavior during the eight-day aquifer test at the study site in Nebraska. Dimensionless head is

$$h_D = 4\pi K_r b(h_0 - h)/Q \tag{16}$$

The solution for the Laplace transform of dimensionless head (Moench and Ogata, 1984) is

$$\bar{h}_D = \frac{K_0(r_D x)}{p} \tag{17}$$

where $\bar{h}_D$ is the Laplace transform of dimensionless head, K_0 is the modified Bessel function of the second kind and order zero, and p is the Laplace transform variable. Furthermore,

$$r_D x = \left\{ \eta^2 + 4\eta\beta' \tanh\left[\frac{4\eta\beta'}{(r/G)^2}\right] + \frac{\eta^2 \operatorname{sech}^2[(4\eta\beta')/(r/G)^2]}{\eta^2\dfrac{(L/b')}{(r/G)^2} + \dfrac{(r/G)^2(Ss'b'/Sy)}{16\beta'^2} + \dfrac{\eta}{4\beta'}\tanh\left[\dfrac{4\eta\beta'}{(r/G)^2}\right]} + 4\eta\beta'' \tanh\left[\frac{4\eta\beta''}{(r/B)^2}\right] \right\}^{1/2} \tag{18}$$

where

$$\eta = (r^2 p / K_r Ss)^{1/2} \tag{19}$$

$$\beta' = \frac{K'_z r}{4K_r b}\left[\frac{K_r\, Ss'}{K'_z Ss}\right]^{1/2} \tag{20}$$

$$\beta'' = \frac{K''_z r}{4K_r b}\left[\frac{K_r Ss''}{K''_z Ss}\right]^{1/2} \tag{21}$$

$$r/G = \frac{r}{b}\left[\frac{K'_z b}{K_r(b' + L)}\right]^{1/2} \tag{22}$$

$$r/B = \frac{r}{b}\left[\frac{K''_z b}{K_r b''}\right]^{1/2} \tag{23}$$

On the right-hand side of (18), the first term represents the drawdown contribution of the aquifer, the second term is the contribution from the water-table aquitard, and the third term is the contribution from the elastic aquitard.

The description of radial flow in the aquifer with an impermeable boundary requires revision of the equations for the aquifer only (A. Moench, written communication, 1986), and (1) now becomes

$$\frac{\partial^2 h}{\partial r^2} + \frac{1}{r}\frac{\partial h}{\partial r} = \frac{Ss}{K_r}\frac{\partial h}{\partial t} + q' - q'' \qquad 0 < r < R \tag{24}$$

where R is the distance from the pumping well to the impermeable boundary. The equation solved for dimensionless drawdown in the Laplace domain is

$$\bar{h}_D = \frac{K_1(R_D x)\, I_0(r_D x)}{p I_1(R_D x)} + \frac{2K_0(r_D x)}{p} \tag{25}$$

where K_1 is the modified Bessel function of the second kind and first order, I_0 is the modified Bessel function of the first kind and zero order, and I_1 is the modified Bessel function of the first kind and first order.

Input for the solution of dimensionless heads at given values of t_D/r_D^2 may be in the form of dimensionless parameters (e.g. β, r/B) or in the form of actual values for individual parameters and ratios of parameters. In this study, actual values and ratios are inserted into (18)–(23) because measurements or estimates have been made for most of the input parameters. Table 2 shows which parameters are input to the solution.

The properties that are specific to the match of a type curve with adjusted drawdown at a given well are: distance to the pumping well; specific yield of the water-table aquitard; and ratios of hydraulic conductivity contrasts between K_r of the aquifer and K'_z or K''_z of each aquitard. Specific yield and hydraulic conductivity ratios were determined by the limited ranges of values for these two parameters (i.e. fitting parameters) that would result in a curve match for a given well.

TABLE 2

Input parameters used in generating three-layer type curves for Type 1 observation wells

Parameter	Notation	Value
Radius of pumping well	r_w	0.3 m
Capillary fringe thickness	L	0.6 m
Water-table aquitard thickness	b'	2.1 m
Aquifer thickness	b	2.3 m
Lower aquitard thickness	b''	107 m
Specific storage, water-table aquitard	Ss'	$7.5 \times 10^{-5}\,m^{-1}$
Specific storage, aquifer	Ss	$7.5 \times 10^{-5}\,m^{-1}$
Specific storage, lower aquitard	Ss''	$5 \times 10^{-5}\,m^{-1}$

Output parameters determined from the curve-matching process are K_r and Ss of the aquifer. Aquitard K'_z values are calculated from K'_z/K_r ratios using the magnitude of K_r determined from curve matching. An example solution is provided below to demonstrate the procedure. Aquifer parameters are calculated from curve matches (Fig. 8) according to

$$K_r = h_D Q/4\pi b(h_0 - h) \tag{26}$$

$$Ss = K_r(t/r^2)/(t_D/r_D^2) \tag{27}$$

For example, for Well 3-SDLC-84 (Fig. 8c) type curve match point coordinates are (100, 10), so $t_D/r_D^2 = 100$ and $h_D = 10$. Match point coordinates are $(2.38 \times 10^{-3}, 0.83)$ for the adjusted drawdown vs. t/r^2 plot for 3-SDLC-84, so $h_0 - h = 0.83$ m and $t/r^2 = 2.38 \times 10^{-3}\,min\,m^{-2}$. Therefore

$$K_r = \frac{10\ (3.4\,m^3\,min^{-1})\ (1\,min/60\,s)}{4\pi\ (2.3\,m)\ (0.83\,m)} = 2.36 \times 10^{-2}\,m\,s^{-1} \tag{28}$$

$$Ss = (2.36 \times 10^{-2}\,m\,s^{-1})\ (2.38 \times 10^{-3}\,min\,m^{-2})\ (60\,s\,min^{-1})/100$$

$$= 3.37 \times 10^{-5}\,m^{-1} \tag{29}$$

Adjusted drawdown curves for Type 1 wells were matched with three-layer type curves starting at ~2.5 min (Fig. 8) because earlier drawdown data were affected by the greater initial pumping rate. Match points and resultant output parameters (calculated as for Well 3-SDLC-84 above) are presented in Table 3 with corresponding input values.

For comparison, adjusted drawdown curves for four Type 1 wells were matched with three-layer type curves including data prior to 2.5 min (Barrash, 1986). Values for Sy are 1.5–3 times larger when data curves are matched to all the early-time data; K_r and K'_z/K_r values differ slightly or not at all. Ss values are up to two times lower to compensate for larger Sy in the system.

Although curve matches are good for early and middle portions of Type 1 wells, departure from the infinite aquifer type curves occurs at about 100–300 min in inner ring wells and at about 400–500 min in middle-ring wells

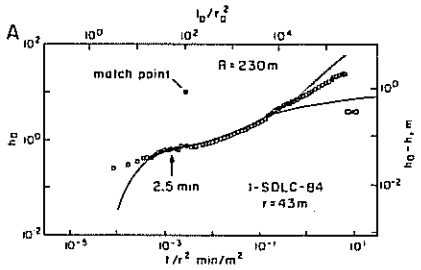
A
match point
R=230m
2.5 min
1-SDLC-84
r=43m

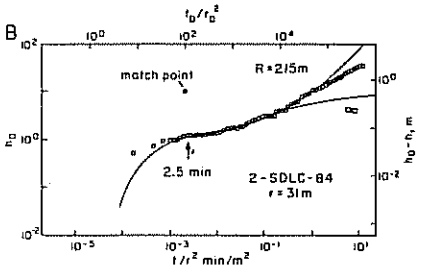
B
match point
R=215m
2.5 min
2-SDLC-84
r=31m

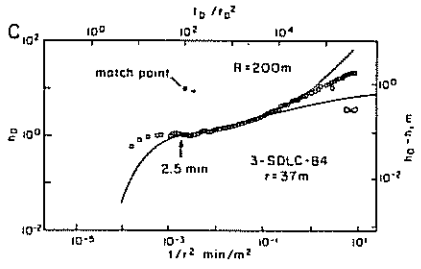
C
match point
R=200m
2.5 min
3-SDLC-84
r=37m

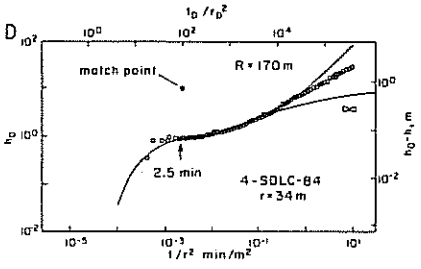
D
match point
R=170m
2.5 min
4-SDLC-84
r=34m

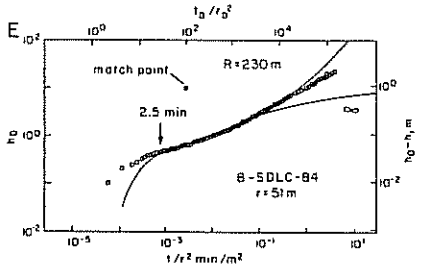
E
match point
R=230m
2.5 min
6-SDLC-84
r=51m

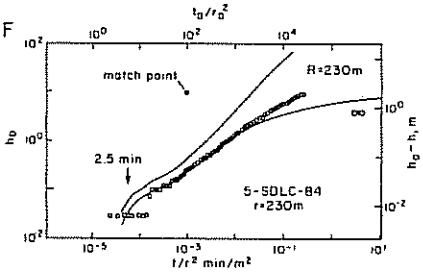
F
match point
R=230m
2.5 min
5-SDLC-84
r=230m

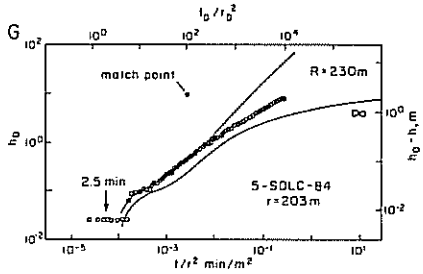
G
match point
R=230m
2.5 min
5-SDLC-84
r=203m

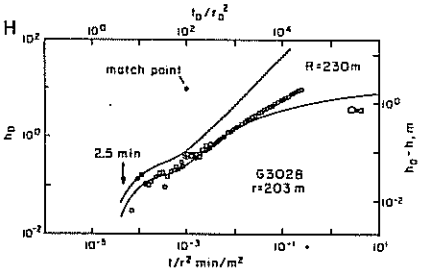
H
match point
R=230m
2.5 min
G3028
r=203m

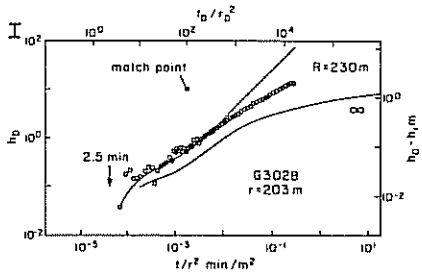
I
match point
R=230m
2.5 min
G3028
r=203m

TABLE 3

Output for infinite aquifer at Type 1 wells

Well	Radius to well (m)	Match point		Sy	K_z'/K_r[a]	K_r ($m\,s^{-1}$)	K_z'[b] ($m\,s^{-1}$)	Ss (m^{-1})
		t/r^2 ($min\,m^{-2}$)	$h_0 - h$ (m)					
1-SDLC-84	43	2.77×10^{-3}	0.82	0.09	0.006	2×10^{-2}	1×10^{-4}	3×10^{-5}
2-SDLC-84	31	2.08×10^{-3}	0.53	0.09	0.006	4×10^{-2}	2×10^{-4}	5×10^{-5}
3-SDLC-84	37	2.38×10^{-3}	0.83	0.14	0.004	2×10^{-2}	1×10^{-4}	3×10^{-5}
4-SDLC-84	34	1.76×10^{-3}	0.76	0.14	0.007	3×10^{-2}	2×10^{-4}	3×10^{-5}
8-SDLC-84	51	2.93×10^{-3}	0.87	0.09	0.006	2×10^{-2}	1×10^{-4}	4×10^{-5}
5-SDLC-84	203	1.06×10^{-3}	2.0	0.11	0.0016	1×10^{-2}	2×10^{-6}	1×10^{-5}
G3028	203	1.04×10^{-3}	1.97	0.11	0.0012	1×10^{-2}	1×10^{-5}	1×10^{-5}

[a]Same as K_z''/K_r.
[b]Same as K_z''. Note also that K_z values are rounded after calculation with unrounded K_r values.

(Fig. 8). Departures from the type curves are interpreted to be leaky boundary effects reflecting the limited areal extent of the major fracture zone.

For the impermeable boundary condition, curve matches were achieved using distances from the pumping well to the impermeable boundary of 170–230 m (Table 4, Fig. 8). All such distances are less than the distance to Well 9-SLDC-84 (353 m) which is the nearest well known to be outside the major fracture zone (Figs. 3 and 9). However, several matches were achieved with distances to the impermeable boundary that are less than the distances from

TABLE 4

Output for an aquifer with an impermeable boundary

Well	Radius to well (m)	Radius to boundary (m)	Match point		Sy	K_z'/K_r[a]	K_r ($m\,s^{-1}$)	K_z'[b] ($m\,s^{-1}$)	Ss (m^{-1})
			t/r^2 ($min\,m^{-2}$)	$h_0 - h$ (m)					
1-SDLC-84	43	230	2.77×10^{-3}	0.82	0.09	0.006	2×10^{-2}	1×10^{-4}	3×10^{-5}
2-SDLC-84	31	215	2.08×10^{-3}	0.53	0.09	0.006	4×10^{-2}	2×10^{-4}	5×10^{-5}
3-SDLC-84	37	200	2.38×10^{-3}	0.83	0.14	0.004	2×10^{-2}	1×10^{-4}	3×10^{-5}
4-SDLC-84	34	170	1.76×10^{-3}	0.76	0.14	0.007	3×10^{-2}	2×10^{-4}	3×10^{-5}
8-SDLC-84	51	230	2.93×10^{-3}	0.87	0.09	0.006	2×10^{-2}	1×10^{-4}	4×10^{-5}
5-SDLC-84	203	230	2.85×10^{-3}	2.25	0.11	0.0016	1×10^{-2}	2×10^{-6}	1×10^{-5}
G3028	203	230	1.87×10^{-3}	1.49	0.11	0.0012	1×10^{-2}	1×10^{-5}	1×10^{-5}

[a]Same as K_z''/K_r.
[b]Same as K_z''. Note also that K_z values are rounded after calculation with unrounded K_r values.

Fig. 8. (A–I) Type curve matches for Type 1 wells for both infinite and laterally bounded aquifer scenarios (allowing for excess drawdown during the first 2.5 min). R is the distance to the lateral boundary used in generating a type curve.

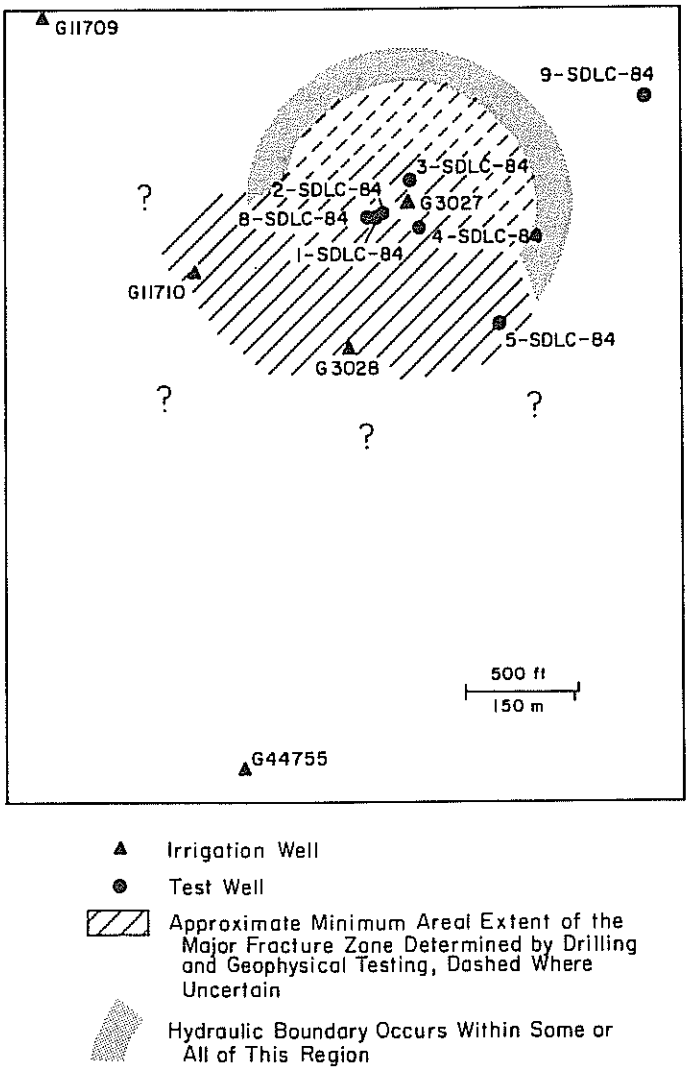

Fig. 9. Extent of major fracture zone as interpreted from type curve analysis and by drilling and borehole geophysical testing.

the pumping well to Wells 5-SDLC-84 and G3028, and all matches used distances to the impermeable boundary that are less than the distance to Well G11710 (< 294 m). This is not necessarily disturbing because the major fracture zone may not be circular in plan view and because the pumping well apparently is not located in the center of the major fracture zone (acknowledged violations of Assumption 3).

It should be noted that impermeable-boundary type curves for middle-ring Wells 5-SDLC-84 and G3028 were generated with low Stehfest numbers (four as

opposed to 12 used in runs for other wells) due to numerical instabilities at higher numbers. Resulting loss of accuracy is limited to the early-time portion of curves, where measured data have the greatest scatter.

A tacit assumption underlying the analytical modeling is that the aquifer remains unsaturated during the period of analysis. However, water levels dropped in the major fracture zone in the pumping well, at least three observation wells (1-, 2-, and 8-SDLC-84), and possibly two other observation wells (G3028 and G11710) during the aquifer test. However, this conversion from confined to unconfined conditions occurred after the time at which effects become negligible (Barrash, 1986), according to the method of analysis developed by Moench and Prickett (1972).

Discussion of results

Parameter outputs from curve matches (Table 3) should be viewed as approximations because of the uncertainties in assumed system characteristics and effects of early-time high and variable pumping rates. In spite of this, the ranges of output values are not great.

Specific yield values of 0.09–0.14 are reasonable because the Brule Formation has a porosity of ~ 0.4 (Barrash, 1986), a large percentage of very small pores, and an abundance of swelling clay (Stanley and Benson, 1979; Retallack, 1983). For comparison, a specific yield of 0.13 was computed by Borchert (1985) in eastern Wyoming by dividing the volume of water pumped by the volume of Brule Formation dewatered during a seven-day period when 14 wells were pumping. Subsequently, Borchert (1985) used 0.10 for the average regional specific yield in model simulations of transient hydrologic behavior in a 337 km^2 area of the LaGrange aquifer (primarily Brule Formation with associated saturated alluvium in places).

Specific storage output values of $1 \times 10^{-5} m^{-1}$ to $5 \times 10^{-5} m^{-1}$ are reasonable for siltstone, and most compare favorably with the calculated estimate of $7.5 \times 10^{-5} m^{-1}$ based on measurements of porosity and compressibility of core samples (Barrash, 1986). However, the output values are not strictly independent confirmation of the calculated estimate because Ss is a 'fixed' input parameter (Table 2) in the mathematical expression for the leakage contribution of the water-table aquitard in (5).

Three types of hydraulic conductivity output are: aquifer K_r, ratio of aquitard K'_z to aquifer K_r, and magnitude of aquitard K'_z or K''_z. Aquifer K_r of 1×10^{-2} to $4 \times 10^{-2} m\,s^{-1}$ is comparable to the more permeable range of gravel (Freeze and Cherry, 1979). The ratio of K'_z/K_r (or K''_z/K_r) ranges from 0.0012 to 0.007. Aquitard K'_z output values are 1×10^{-5} to $2 \times 10^{-4} m\,s^{-1}$; these values are calculated from K_r and K'_z/K_r for each well (Table 3). The K'_z output values are two to three orders of magnitude larger than K'_z values measured on siltstone core *without* secondary permeability features (Barrash, 1986; Barrash and Morin, 1987).

Although both aquifer K_r and aquitard K'_z are relatively large, several

factors should be considered when assessing the reasonableness of these hydraulic conductivity values. With respect to aquifer K_r, a large discharge rate was sustained for eight days with low drawdown and hydraulic gradients (Table 1), lost circulation occurred during drilling, and a dense fracture network is evident (Fig. 2e–f). With respect to aquitard K'_z: (1) non-tectonic secondary permeability (especially the presence of pedotubules) is widespread in the tested Brule Formation section (Fig. 2a–c), but was *not* represented in core samples measured for permeability (Barrash, 1986; Barrash and Morin, 1987); (2) secondary permeability due to tectonic(?) joints may enhance vertical hydraulic conductivity in the aquitard; (3) subhorizontal parting planes (Fig. 2d) probably increase the interconnections between subvertical secondary permeability features.

Output values of hydraulic conductivity and specific storage for the three layers at the middle-ring wells are consistently less than at the inner-ring wells. Such differences may reflect areal differences in these parameters, perhaps due to changes in the major fracture zone towards the south. Numerical modeling, in progress, will test this hypothesis.

Sensitivity

The output values from curve matching (Tables 3 and 4) are not unique because a number of input values are assumed. To test the effect of changes in inputs, curve matches were obtained using a sample of four Type 1 wells: 2-, 3-, and 4-SDLC-84, and G3028. The match procedure followed for sensitivity analysis was the same as used previously, and input values are the same as in Table 2, except for the factor(s) being evalutated (Table 5).

In general, changes in thickness of layers to reasonable maximum or minimum values do not cause significant changes in output parameter values. However, using a minimal aquifer thickness results in a specific storage at Well G3028 that is nearly two orders of magnitude smaller than that estimated from measurements on core samples. Decreases of lower aquitard thickness to 23 m (stratigraphic location of increased frequency of claystone layers in the Brule Formation) or 61 m (an arbitrary value) result in decreases of specific yield by 50% or more.

Increases and decreases of Sy by about a factor of two result in, respectively, lengthening and shortening the delayed yield portions of type curves such that acceptable matches are not possible. Similarly, increases and decreases of hydraulic conductivity contrast (K'_z/K_r) result in marked flattening or steepening of slope (respectively) in the post-delayed-yield portion of type curves such that curve matches are not possible. However, varying Sy and K'_z/K_r together allows curve matches in systems with (1) Sy decreased by 33–50% and K'_z/K_r decreased by 33–50%, or (2) Sy increased by 100% and K'_z/K_r increased by 12% to nearly 100%. The Sy value of 0.1, then, is a central value within a range of about 0.05–0.15.

Neither increases nor decreases of aquifer Ss by an order of magnitude result

TABLE 5

Parameter values used in sensitivity analysis

Parameter	Initial values	Alternate values	
Capillary fringe thickness, m	0.6	0.3	1.2
Water-table aquitard thickness, m	2.1	1.0	3.0
Aquifer thickness, m	2.3	1.0	3.3
Lower aquitard thickness, m	107	23	61
Water-table aquitard specific yield			
2-SDLC-84	0.09	0.05	0.20
3-SDLC-84	0.14	0.07	0.20
4-SDLC-84	0.14	0.07	0.20
G3028	0.11	0.05	0.20
Aquifer specific storage, m^{-1}	7.5×10^{-5}	7.5×10^{-4}	7.5×10^{-6}
Specific storage, all units, m^{-1}	$Ss' = Ss = 7.5 \times 10^{-5}$	7.5×10^{-4}	7.5×10^{-6}
	$Ss'' = 5 \times 10^{-5}$	5×10^{-4}	5×10^{-6}
Hydraulic conductivity contrast, K'_z/K_r			
2-SDLC-84	0.006	0.01	0.003
3-SDLC-84	0.004	0.01	0.002
4-SDLC-84	0.007	0.01	0.003
G3028	0.0012	0.002	0.0006
Distance to impermeable boundary, m			
2-SDLC-84	215	105	300
3-SDLC-84	200	105	300
4-SDLC-84	170	105	300
G3028	230	105	300

in significant differences in output for other parameters, and these increases or decreases are reflected in *Ss* output calculated from curve matches. The minor influence of such apparently major changes may not be surprising considering the small thickness of the aquifer compared with the three-layered system as a whole.

Increasing or decreasing the input magnitude of *Ss* for all three layers by an order of magnitude requires a parallel increase or decrease of *Sy* by an order of magnitude in the same direction to achieve curve matches. Match points are identical to those of the original solution. Thus, output *Ss* for all layers is now an order of magnitude less or more than that which is used for input. Therefore, despite good type curve fits to the data, the consistent input and output values for *Ss* indicate that these matches are not valid for order of magnitude changes in *Ss* and *Sy*.

Changes in distance to the impermeable boundary of the aquifer cause the predictable results of departures from the late-time portion of drawdown curves either too soon (with decreased distance) or too late (with increased distance).

SUMMARY AND CONCLUSIONS

An aquifer test was conducted to determine the hydraulic behavior of the Brule Formation including a highly conductive, secondary permeability zone

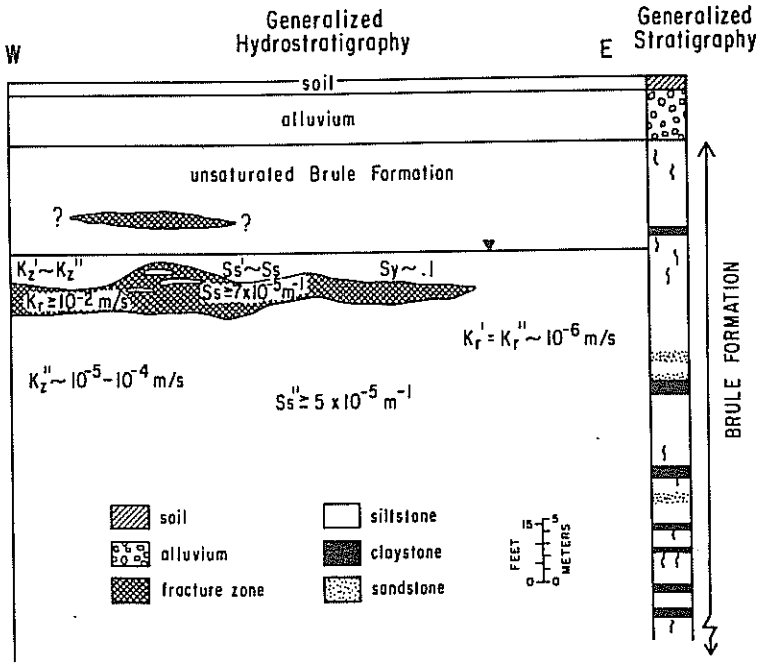

Fig. 10. Summary of hydrostratigraphy with estimates of hydraulic parameters at the scale of the aquifer test, except K'_r and K''_r which were estimated from straddle-packer injection tests.

in Cheyenne County, Nebraska. Results from a variety of field, laboratory and analytical techniques used to investigate the Brule Formation at several volume scales (Barrash and Morin, 1985, 1987; Barrash, 1986; Morin and Barrash, 1986) provide independent but complementary sets of data which are integrated into a consistent, quantitative characterization of the hydrogeological system at the study site. Significant elements of this characterization are illustrated in Fig. 10 and noted below.

(1) The Brule Formation is predominantly siltstone with thin beds of claystone and sandstone. Pedotubules enhance vertical permeability; subhorizontal parting planes enhance horizontal permeability and may integrate pedotubules with a subvertical fracture fabric of tectonic(?) origin.

(2) A subhorizontal, laterally limited region of densely fractured siltstone (major fracture zone) may be one 'layer' or several 'layers' of fractured siltstone in close vertical proximity.

(3) Two types of transient hydraulic response occurred in observation wells monitored during an eight-day aquifer test. Type 1 wells responded rapidly to the initiation and cessation of pumping and had similar magnitudes of drawdown throughout the test; these wells intercepted the major fracture zone and were < 300 m from the pumping well. Type 2 wells had delayed reponses to the initiation and cessation of pumping and markedly less drawdown than Type 1 wells; Type 2 wells do not intercept the fracture zone and are > 300 m from the pumping well.

(4) Transient hydraulic behavior of the Brule Formation at the study site is consistent with a leaky three-layered system with: (i) a water-table aquitard of relatively unfractured Brule Formation; (ii) an aquifer of intensely fractured siltstone; (iii) a lower elastic aquitard of relatively unfractured Brule Formation; (iv) vertical hydraulic conductivity significantly greater than horizontal hydraulic conductivity in the aquitards.

ACKNOWLEDGMENTS

Phyllis Baird generously allowed the use of her farm for a variety of field tests, including the aquifer test described in this paper. This study was supported by a cooperative agreement between the South Platte Natural Resources District and the Conservation and Survey Disivion (CSD) of the University of Nebraska–Lincoln while Warren Barrash was with CSD. An earlier version of this manuscript was reviewed by R. Cooley, I. Javandel, and A. Moench.

REFERENCES

Barenblatt, G.E., Zheltov, I.P. and Kochina, I.N., 1960. Basic concepts in the theory of seepage of homogenous liquids in fissured rocks (strata). J. of Appl. Math. Mech. (USSR), 24(5): 1286–1303.

Barrash, W., 1986. Hydrostratigraphy and Hydraulic Behavior of Fractured Brule Formation in Sidney Draw, Cheyenne County, Nebraska. Ph.D. Thesis, University of Idaho, Moscow, 205 pp.

Barrash, W. and Morin, R.H., 1985. Hydrostratigraphic characterization of fractured Brule

Formation in western Nebraska using geological, geophysical, and hydrological techniques. EOS (Trans. Am. Geophys. Union), 66(46): 891 (abstract).

Barrash, W. and Morin, R.H., 1987. Hydrostratigraphy and distribution of secondary permeability in the Brule Formation, Cheyenne County, Nebraska. Geol. Soc. Am. Bull. 99(4): 445–462.

Barrash, W. and Ralston, D.R., 1988. Analytical modeling of a fracture zone in the Brule Formation as an aquifer receiving leakage from water-table and elastic aquitards. EOS (Trans. Am. Geophys. Union), 69(18): 566 (abstract).

Borchert, W.B., 1985. The ground-water system in the LaGrange aquifer near LaGrange, southeastern Wyoming. U.S. Geol. Surv., Water-Resources Investigations Report 83-4024, 56 pp.

Cooley, R.L. and Case, C.M., 1973. Effect of a water table aquitard on drawdown in an underlying pumped aquifer. Water Resour. Res. 9(2): 434–447.

Freeze, R.A. and Cherry, J.A., 1979. Groundwater. Prentice-Hall, Englewood Cliffs, NJ, 604 pp.

Hantush, M.S., 1960. Modification of the theory of leaky aquifers. J. Geophys. Res. 65(11): 3713–3725.

Long, J.C.S., Remer, J.S., Wilson, C.R. and Witherspoon, P.A., 1982. Porous media equivalents for networks for discontinuous fractures. Water Resour. Res. 18(3): 645–658.

Moench, A.F. and Ogata, A., 1984. Analysis of constant discharge wells by numerical inversion of Laplace transform solutions. Groundwater Hydraulics, Water Resources Monograph Series, 9: 146–170.

Moench, A.F. and Prickett, T.A. 1972. Radial flow in an infinite aquifer undergoing conversion from artesian to water table conditions. Water Resour. Res., 8(2): 494–499.

Morin, R.H. and Barrash, W., 1986. Defining patterns of ground water and heat flow in fractured Brule formation, western Nebraska, using borehole geophysical methods. Proceedings of the NWWA Conference on Surface and Borehole Geophysical Methods and Ground Water Instrumentation, Denver, CO, October 15–17, pp. 545–569.

Retallack, G.J., 1983. Late Eocene and Oligocene paleosols from Badlands National Park, South Dakota. Geol. Soc. Am., Spec. Pap., 193, 82 pp.

Stanley, K.O. and Benson, L.V., 1979. Early diagenesis of High Plains Tertiary vitric and arkosic sandstone, Wyoming and Nebraska. Soc. Econ. Paleontol. Mineral., Spec. Publ., 26: 401–423.

Stehfest, H., 1970. Numerical inversion of Laplace transforms. Commun. ACM, 13(1): 47–49.